communications biology

Article

https://doi.org/10.1038/s42003-024-06638-z

Aberrant neural computation of social controllability in nicotine-dependent humans

Caroline McLaughlin[1,2,3], Qi Xiu Fu[1,2,3], Soojung Na[1,2,3], Matthew Heflin[2,3], Dongil Chung[4], Vincenzo G. Fiore[2,3] & Xiaosi Gu[1,2,3]

Social controllability, or the ability to exert control during social interactions, is crucial for optimal decision-making. Inability to do so might contribute to maladaptive behaviors such as smoking, which often takes place in social settings. Here, we examined social controllability in nicotine-dependent humans as they performed an fMRI task where they could influence the offers made by simulated partners. Computational modeling revealed that smokers under-estimated the influence of their actions and self-reported a reduced sense of control, compared to non-smokers. These findings were replicated in a large independent sample of participants recruited online. Neurally, smokers showed reduced tracking of forward projected choice values in the ventromedial prefrontal cortex, and impaired computation of social prediction errors in the midbrain. These results demonstrate that smokers were less accurate in estimating their personal influence when the social environment calls for control, providing a neurocomputational account for the social cognitive deficits in this population. Pre-registrations: OSF Registries|How interoceptive state interacts with value-based decision-making in addiction (fMRI study). OSF Registries|COVID-19: social cognition, mental health, and social distancing (online study).

For humans, our social environment presents the most challenging situation for exerting behavioral control, due to its high degree of complexity and uncertainty. *Social controllability*, defined as one's ability to exert control during interpersonal interactions, is thus essential for optimal decision-making in everyday scenarios[1]. Disruptions in this ability might lead to suboptimal behaviors such as drug abuse, which is often intertwined with social dynamics. Notably, smoking and nicotine use exemplify highly social activities, particularly prevalent among younger adults[2,3]. While prior work has examined various constructs related to nicotine addiction (e.g., cue reactivity, impulsive control), little is known regarding the mechanisms underlying social cognitive deficits in nicotine-dependent humans. Specifically, understanding the distinction in how human smokers exert and perceive social control compared to non-smokers at both neural and computational levels remains elusive.

Previously, reinforcement learning (RL) algorithms have been used to capture how drugs might alter neural computations underlying decision-making, such as the encoding of reward prediction errors by the mesolimbic circuit[4–6]. Furthermore, economic preference models such as temporal discounting have also revealed that substance-dependent individuals show a preference for smaller immediate rewards over delayed larger rewards[7–9] which may reflect a complex interaction between cognitive control, time perception, and risk preference[10–12]. More recent computational models have linked addiction to dysfunctions in model-based control[13,14] and forward planning[15–17]. Others have postulated that these model-based planning deficits in addiction are further amplified by complex environments[18,19]. However, empirical evidence supporting these computational frameworks in substance-dependent humans - especially in the context of social decision-making - is still scarce. Here, we aim to directly examine the neural computations underlying social controllability in substance-dependent humans (smokers v.s. non-smokers), using a computational psychiatry approach and nicotine addiction as a test case.

Based on the literature reviewed thus far, we hypothesized that smokers would demonstrate reduced ability to exert social control, subserved by reduced neural computations of social forward planning signals. At the neural level, previous work shows that the ventromedial prefrontal cortex (vmPFC) is important for tracking the downstream effects of human agents'

[1]Department of Neuroscience, Icahn School of Medicine at Mount Sinai, New York, NY, USA. [2]Department of Psychiatry, Icahn School of Medicine at Mount Sinai, New York, NY, USA. [3]Center for Computational Psychiatry, Icahn School of Medicine at Mount Sinai, New York, NY, USA. [4]Department of Biomedical Engineering, Ulsan National Institute of Science and Technology, Ulsan, Republic of Korea. e-mail: xiaosi.gu@mssm.edu

current choices in order to exploit the controllability of a simulated social environment in healthy volunteers[1]. The vmPFC has been consistently shown to encode cognitive maps, an efficient way to represent task space and environmental structure that are crucial for model-based planning[20]. Using a similar decision-making task (Fig. 1) in smokers and non-smokers across two independent samples (in-person fMRI sample: $n = 17$ for smokers and $n = 25$ for non-smokers; online replication sample: $n = 72$ for smokers and $n = 147$ for non-smokers; see *Methods* and Supplementary Tables S1, S2 for participant characteristics), the current study examined how vmPFC-dependent social controllability computation might differ between nicotine-dependent human smokers and non-smokers. Participants made choices about accepting or rejecting monetary proposals from simulated partners (i.e., the ultimatum game; Fig. 1a); crucially, and different from the typical ultimatum game, their choices could increase or decrease the future monetary proposals from the partners in a probabilistic fashion (Fig. 1b). We used computational modeling (see *Methods*) to quantify a key parameter δ ("estimated influence") representing the mentally simulated influence of one's actions on future social outcomes[1]. We predicted that smokers would underestimate the level of influence their actions have on the future, compared to controls, accompanied by reduced neural activation in the vmPFC. A secondary analysis will also examine neural activations (e.g., midbrain) related to social prediction errors in both groups.

Results

Smokers failed to exploit the controllability of their social interactions

We first evaluated model-agnostic measures of participants' behaviors to determine their ability to detect and exploit the controllability of their interactions with simulated partners in this task, indexed by the offer amount they obtained. Compared to non-smokers who successfully raised the offers over time (Fig. 2a), smokers were unable to exploit the controllability of their interactions, indexed by the flat or slightly decreasing offer sizes over time (Fig. 2b). On average, smokers received lower offers ($4.5 ± 2.14) compared to controls ($5.98 ± 1.95; $t(40) = 2.31$, $p = 0.0131$; Cohen's $d = -0.72$; Fig. 2b). This suggests that overall, smokers failed to exploit the controllability of their social environment.

Given the contingencies designed in the game, participants would need to strategically reject smaller offers to raise future ones. Thus, we compared rejection rates between smokers and non-smokers. While total rejection rates were not significantly different between smokers (43.23% ± 23.75) and non-smokers (50.26% ± 14.79; $P > 0.05$; Cohen's $d = -0.35$) (Fig. 2c), smokers exhibited lower rejection rates (46.72% ± 33.53) for medium sized ($4–$6) offers compared to non-smokers (66.93% ± 33.20; $t(40) = 2.27$, $p = 0.0144$; Cohen's $d = -0.61$); Fig. 2d. There were no significant differences for low ($1–$3) or high ($7–$9) offers. This finding suggests that a lack of strategic rejection of medium sized offers contributed to smokers' inability to raise offers overall.

Although smokers reported a lower sense of control (52.40% ± 20.76) compared to non-smokers (65.91% ± 22.39; $t(37) = -1.93$, $p = 0.062$; Cohen's $d = -0.63$; Fig. 2e), this difference was not statistically significant (potentially due to the small sample size; due to technical failures, sense of control ratings for three non-smoker participants were also missing). Taken together, these model-agnostic behavioral results reveal impaired social controllability in smokers, primarily indexed by their reduced ability to raise offers in the Controllable condition.

Smokers under-estimated the influence of their current choices on future interactions

Next, we sought to uncover the computational mechanisms underlying participants' choices using a series of models including various depths of forward thinking (FT) computations (1 to 4) while accounting for norm violation in subjective utility, a model not involving FT but still considering norm violation (0-step), and a model solely relying on cached value in a model-free fashion without forward thinking or norm violation (model-free reinforcement). Model comparison results demonstrated that in the controllable condition, all the FT models better explained both smokers' and non-smokers' choices compared to the 0-step or model-free RL model (Table S3). Consistent with our previous work, the 2-step FT model also showed good parameter recoverability (Tables S4, S5) and was selected for subsequent statistical and neural analyses. Overall, the 2-step FT model predicted non-smokers' choices with an 86.21% accuracy (Fig. 3b) and smokers' choices with an 86.47% accuracy (Fig. 3c).

Next, we examined parameters from the 2-step model (see Table 1 for all parameter values). Our key parameter of interest here is δ, representing the mentally estimated controllability or influence of one's current choices on future offers. We found a significant difference in this parameter between

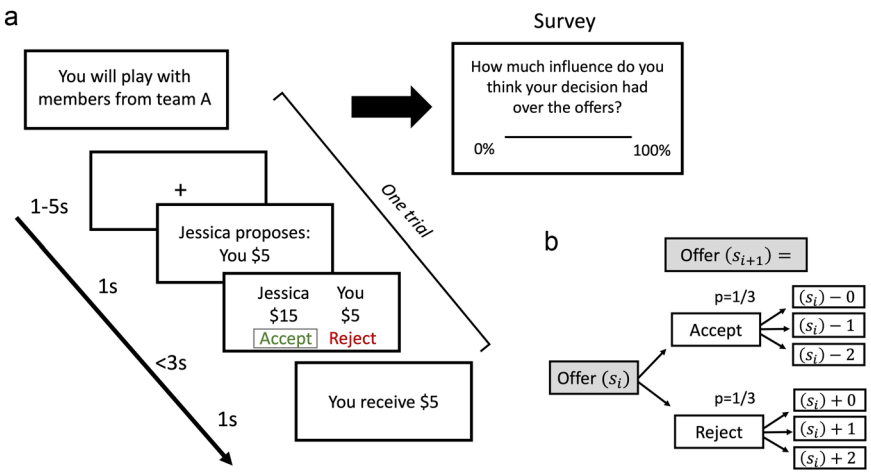

Fig. 1 | Experimental paradigm. a Participants played the social controllability task. At the start of the task, participants were only informed about the team with whom they were playing but not how the teams differed in terms of their social controllability. As such, they would need to learn the contingencies between their actions and consequences during their interactions with each team. Within the same block, they played with different virtual individuals from the same team for each trial. Participants' main goal is to decide whether to accept or reject an unfair offer from a virtual team member proposing how to divide $20. If the participant accepts, both partners will receive the proposed amount. If the participant rejects, both partners will receive $0. At the end of the game, participants rated their perceived controllability over their interactions for each team. **b** A schematic of contingencies for the controllable condition of the task displays how the following offer was generated based on the participant's previous action. If participants accepted the current offer (s_i), the subsequent offer (s_{i+1}) decreased by $0, $1, $2 with a 1/3 probability for each. If they rejected the current offer (s_i), the subsequent offer (s_{i+1}) increased by $0, $1, $2 with a 1/3 probability for each.

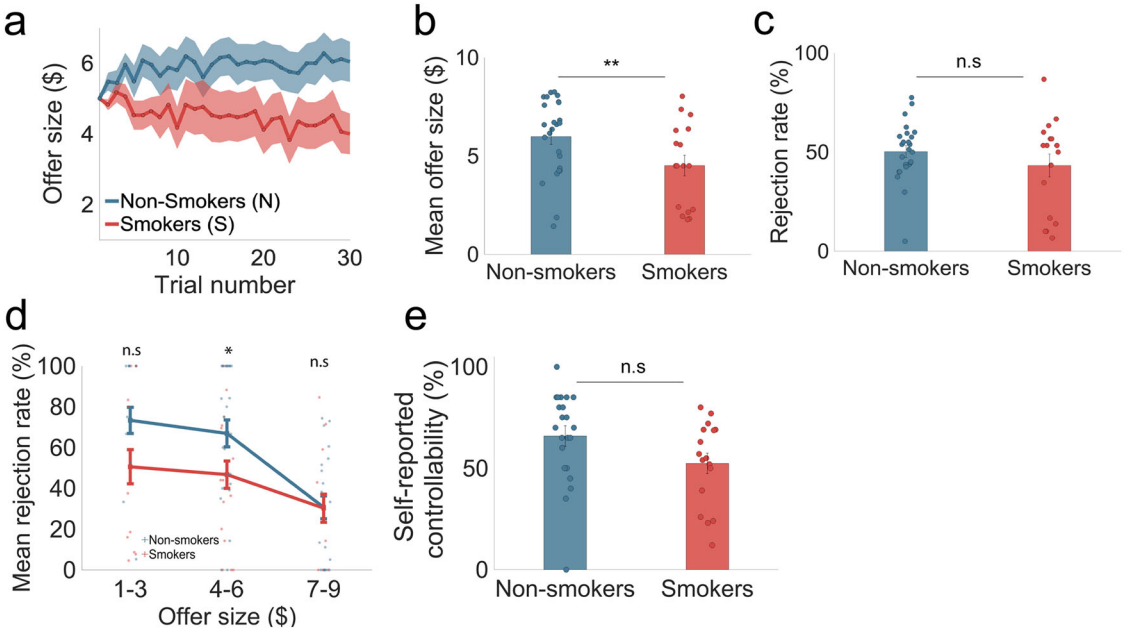

Fig. 2 | Smokers failed to exploit the controllability of controllable social interactions compared to non-smokers (in-person fMRI sample). In the controllable condition of the task, (**a**) smokers' offer sizes ($n = 17$) slightly decrease from trial to trial while non-smokers' ($n = 25$) offer sizes increase from trial to trial. Shaded patches indicated SEM. **b** A two-sampled t-test revealed that individual mean offer sizes are significantly lower for smokers ($4.5 ± 2.14) compared to non-smokers ($5.98 ± 1.95; $t(40) = 2.31$, $p = 0.0131$; Cohen's $d = -0.72$). Error bars indicate SEM. **c** Overall rejection rate was not significantly different for smokers (43.23% ± 23.75) compared to non-smokers (50.26% ± 14.79; $p > 0.05$; Cohen's $d = 0.35$). Error bars indicate SEM. **d** However, when rejection rates were divided and categorized by low ($1–$3), medium ($4–$6) and high ($7–$9) offers, smokers had a significantly lower rejection rate for medium offer sizes (46.72% ± 33.53) compared to non-smokers (66.93% ± 33.20; $t(40) = 2.27$, $p = 0.0144$; Cohen's $d = -0.61$). Error bars indicate SEM. **e** Perceived controllability rated on a scale of 1% to 100% after each condition of the task was not significantly different between smokers (52.40% ± 20.76) and non-smokers (65.91% ± 22.39; $t(37) = 1.93$, $p = 0.062$; Cohen's $d = -0.63$). Error bars indicate SEM. For figure source data refer to (Supplementary Data 1).

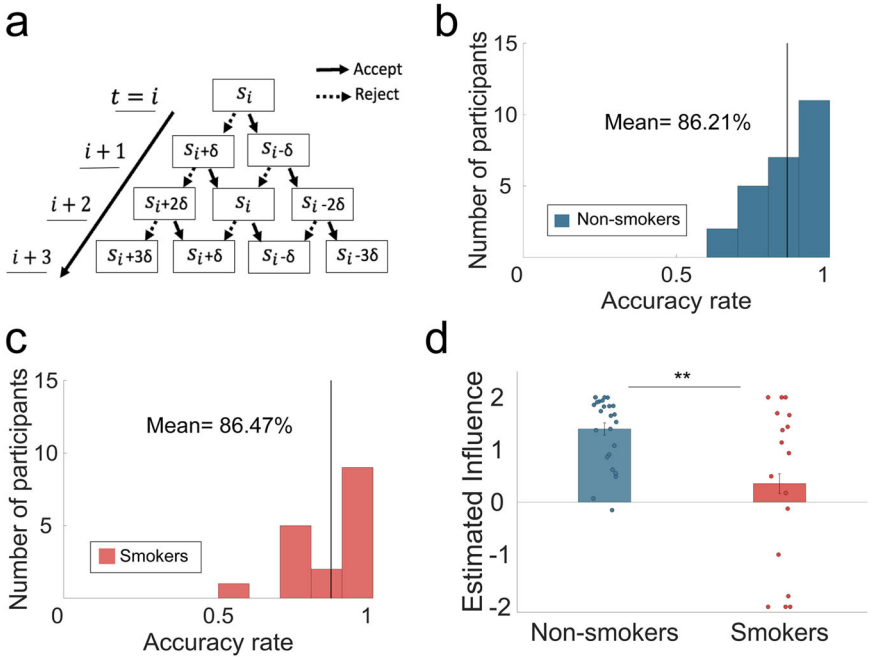

Fig. 3 | A computational model of forward thinking (FT) revealed that smokers were able to mentally simulate future interactions, but inaccurately underestimated their influence on future offers (in-person fMRI sample). a A schematic demonstrating how an agent might mentally simulate the values of future states using a forward thinking model. Simulated offers increase or decrease by estimated influence δ, dependent on participants' choice to accept or reject the split of money. **b** The 2-step model of FT predicted non-smokers' choice in the 'Controllable' condition of the task with a mean accuracy rate of 86.21% (bold black line). **c** The 2-step model of FT predicted smokers' choice in the 'Controllable' condition of the task with a mean accuracy rate of 86.47%. **d** The parameter of interest, estimated influence, estimated from the 2-step FT model in the 'Controllable' condition of the task was significantly lower for nicotine- smokers (0.352 ± 1.54) compared to non-smokers (1.40 ± 0.654; $t(40) = -3.02$, $p = 0.002$; Cohen's $d = 0.89$). Error bars indicate SEM. For figure source data refer to (Supplementary Data 1).

Table 1 | Parameter estimates from the 2-step forward thinking model

	Inverse temperature β	Sensitivity to norm violation α	Initial norm μ	Adaptation rate ε	Estimated influence δ
fMRI Sample					
Non-smokers	8.814 (8.464)	0.687 (0.313)	8.342 (7.555)	0.171 (0.160)	1.396 (0.654)
Smokers	9.172 (7.662)	0.699 (0.411)	10.517(7.478)	0.284 (0.338)	0.352 (1.544)
t-value	0.14	0.105	0.92	1.454	−3.018
p value	0.445	0.458	0.182	0.077	0.002**
Online Sample					
Non-smokers	9.032 (8.498)	0.754 (0.238)	8.418 (6.994)	0.336 (0.295)	1.351 (0.833)
Smokers	9.206 (8.737)	0.743 (0.311)	9.871 (7.883)	0.306 (0.315)	1.119 (1.016)
t-value	−0.140	0.269	−1.328	0.679	1.677
p value	0.438	0.388	0.093	0.253	0.045*

Mean (SD) of parameters estimated in the model include inverse temperature, sensitivity to norm violation, initial norm, adaptation rate and estimated influence (parameter of interest). Statistics for the fMRI sample (non-smokers $n = 17$; smokers $n = 25$) are obtained through a two-sample t-test, while the online sample (non-smokers $n = 147$; smokers $n = 72$) utilizes a non-parametric bootstrapping test.

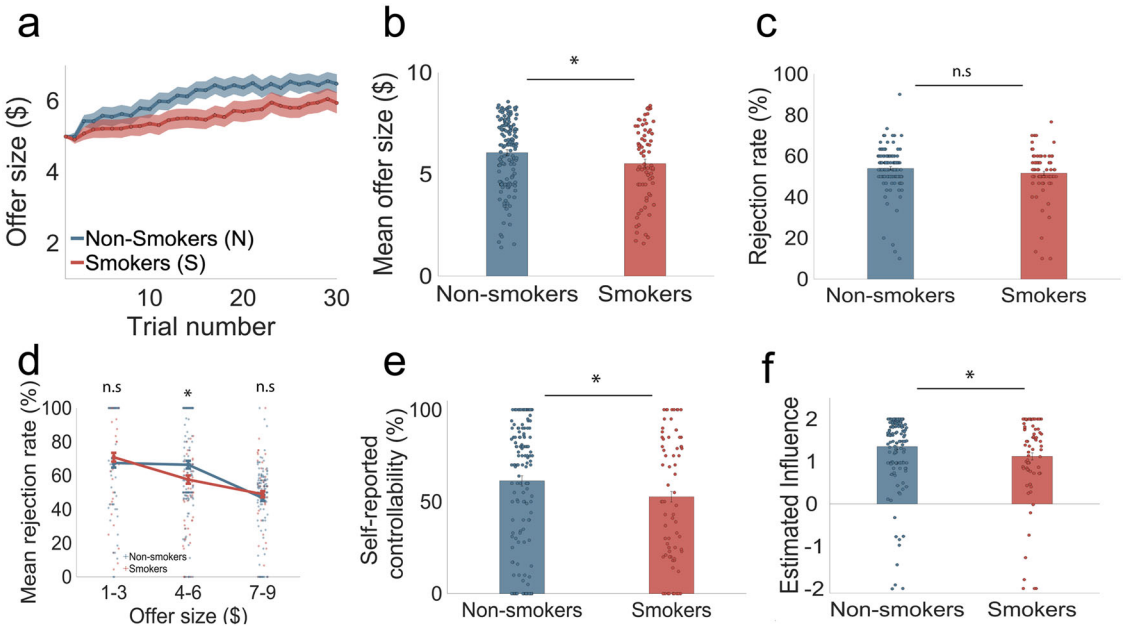

Fig. 4 | Replication study: smokers perceived and inaccurately under-estimated the influence of their current choices on future interactions in an independent online sample. In the controllable condition of the task (**a**) smokers' ($n = 72$) offers increased trial-by-trial but remained below non-smokers'($n = 147$) offer sizes. Shaded patches indicated SEM. **b** A non-parametric test shows that mean offer sizes were significant lower for smokers ($5.53 ± 1.85) compared to non-smokers ($6.06 ± 1.68; $p = 0.0266$; Cohen's $d = -0.30$). Error bars indicate SEM. **c** Overall rejection rates were not significantly different between smokers (51.57 ± 12.36) and non-smokers (53.97% ± 9.85; $p > 0.05$; Cohen's $d = -0.21$). Error bars indicate SEM. **d** However, when rejection rates were divided and categorized by low ($1–$3), medium ($4–$6) and high ($7–$9) offers, a non-parametric bootstrapping test shows that smokers had a significantly lower rejection rate for medium offer sizes (57.59% ± 29.34) compared to non-smokers (66.40% ± 27.24; $p = 0.0175$; Cohen's $d = -0.31$). **e** Perceived controllability rated on a scale of 1% to 100% after each condition of the task was significantly lower among smokers (52.68% ± 34.46) compared to non-smokers (61.32% ± 34.63; $p = 0.0442$; Cohen's $d = -0.25$). Error bars indicate SEM. **f** The parameter of interest, estimated influence, estimated from the 2-step forward thinking model in the 'Controllable' condition of the task, was significantly lower for smokers (1.119 ± 1.016) compared to non-smokers (1.351 ± 0.833; $p = 0.0447$; Cohen's $d = 0.25$). Error bars indicate SEM. For figure source data refer to (Supplementary Data 1).

smokers (0.352 ± 1.54) and non-smokers (1.40 ± 0.654; $t(40) = -3.02$, $p = 0.002$; Cohen's $d = -0.89$; Fig. 3d).

There was no order effect on delta in either group ($Ps > 0.1$; see *Supplementary Results*), similar to our previous results[1]. This result suggests that while engaging a 2-step forward thinking model, smokers significantly underestimated the potential impact of their current choices on future interactions compared to non-smokers. No other parameters showed a significant difference between groups. These findings suggest that a lower δ – a reduced estimate of influence of one's actions on the environment – serves a candidate computational substrate for impaired controllability observed in smokers.

Replication of behavioral and computational results in an independent online sample

Next, we analyzed data collected from an independent online sample of smokers and non-smokers to assess the generalizability of the behavioral and computational findings observed in the in-person fMRI study (see Table S2 for online participants' characteristics). In line with findings from the in-

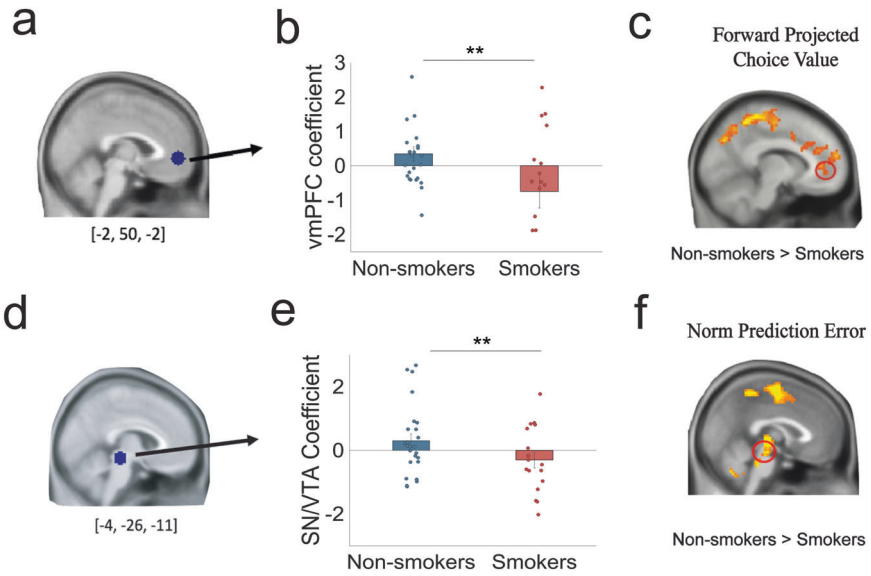

Fig. 5 | Smokers show unusual ventromedial prefrontal cortex (vmPFC) and midbrain activity while computing forward projected choice values and norm prediction errors, respectively. **a** vmPFC ROI coefficient [−2, 50, −2] was selected from an independent study[23] and extracted from an 8-mm radius sphere for estimated choice values from the 2-step forward thinking model in the controllable condition of the task ($P_{FDR} < 0.05$, $k > 50$). **b** vmPFC coefficients were significantly greater for non-smokers (0.347 ± 1.05) compared to smokers (−0.749 ± 2.00; $t(40) = -2.31$, $p = 0.013$; Cohen's $d = 0.69$). Error bars indicate SEM. **c** One-way between-subject ANOVA test for the whole-brain map further revealed that BOLD responses in the vmPFC is greater for non-smokers compared to smokers ($P_{FDR} < 0.05$ and $k > 50$). **d** The midbrain ROI coefficient [−4, −26, −11], covering the substantia nigra (SN) and ventral tegmental area (VTA), were selected from an independent study[27] and extracted for norm prediction errors from the 2-step forward thinking model in the controllable condition of the task. **e** SN/VTA coefficients were significantly greater for non-smokers (0.302 ± 1.10) compared to smokers (−0.306 ± 1.04; $t(40) = -1.80$, $p = 0.040$; Cohen's $d = 0.57$). Error bars indicate SEM. **f** One-way between-subject ANOVA test for the whole-brain map further revealed that neural responses to norm prediction errors in the midbrain was greater for non-smokers compared to smokers ($P_{FDR} < 0.05$ and $k > 50$). For figure source data refer to (Supplementary Data 1).

person sample, smokers recruited online also exhibited reduced offer sizes over time compared to non-smokers, albeit with a slightly upward trend in their offer trajectory (Fig. 4a). On average, smokers still received significantly lower offers (5.53 ± 1.85) compared to non-smokers (6.06 ± 1.68; bootstrapping $p = 0.0266$; Cohen's $d = -0.30$; Fig. 4b), although this effect size was smaller than the in-person study. These findings highlight that smokers recruited online, similar to those recruited in-person, were less successful than non-smokers at exploiting the controllability of the social environment.

Consistent with our in-person sample, we found no significant differences in total rejection rates between smokers (51.57% ± 12.36) and non-smokers (53.97% ± 9.85) ($p = 0.077$; Cohen's $d = -0.21$; Fig. 4c). Nevertheless, when we analyzed rejection rates based on offer size (low: $1–$3, medium: $4–$6, and high: $7–$9), we replicated the previously observed pattern of lower rejection rates among smokers for medium offers (smokers: 57.59% ± 29.34, non-smokers: 66.40 ± 27.24; $p = 0.0175$; Cohen's $d = -0.31$; Fig. 4d). Leveraging the existence of an independent risky decision-making task in this cohort[21], we then tested whether the group difference in rejection rate observed here were attributable to individual differences in risk aversion (see *Supplementary Methods* for details). To this end, we constructed GLMs with risk aversion parameter values estimated from this task[22] as an independent variable to predict rejection rate. This analysis demonstrated that risk aversion did not underpin the observed differences in rejection rates (for medium-sized offers) between the subject groups (Table S8).

Finally, online smokers self-reported a significantly reduced sense of control than online non-smokers (smokers: 52.68% ± 34.46, non-smokers: 61.32% ± 34.63; $p = 0.0442$; Cohen's $d = -0.25$; Fig. 4e), despite a smaller effect size compared to the in-person study. Taken together, these model-agnostic analyses of a much larger and variable online sample provided converging evidence that smokers showed impairments in their ability to exploit the controllability of their social interactions, indexed by reduced ability to raise offers in the Controllable condition. We also found that group differences in perceived controllability ratings diverged between in-person and online samples, reflecting the huge variability in subjective perception.

Next, we applied the same computational models to fit the choice data collected from online participants. Overall, model-based results were also consistent between the in-person and online sample. Specifically, we found that the estimated influence parameter from the 2-step model was significantly reduced in smokers (1.12 ± 1.02) compared to non-smokers (1.35 ± 0.83; $p = 0.0447$; Cohen's $d = 0.25$; Fig. 4f). Similar to our in-person sample and previous study[1], we did not observe any order effects on the estimated controllability parameter ($Ps > 0.2$; see *Supplementary Results*). Furthermore, this effect could not be attributed to mood symptoms (assessed by Beck Depression Inventory-II; Table S6) or impulsivity tendencies (assessed by Barratt Impulsivity Scale) commonly associated with addiction (Table S7).

These findings collectively indicate that the larger online sample replicated key behavioral and computational findings observed in the in-person study, thereby further confirming aberrant forward thinking in smokers across a wide range of severity.

Smokers showed aberrant encoding of forward thinking value in the vmPFC

For the neural analyses, our primary focus was to examine neural activities associated with the forward thinking value signal, found to be encoded by the vmPFC in non-smokers[1]. Thus, we initially conducted ROI analysis using beta coefficients extracted from an independent ROI of the vmPFC [−2, 50, −2][23] (Fig. 5a). This analysis revealed that vmPFC activations related to total choice value were significantly greater for non-smokers (parameter estimate: 0.347 ± 1.05) compared to smokers (parameter estimate: −0.749 ± 2.00; two-sample $t(40) = -2.31$, $p = 0.013$; Cohen's $d = 0.69$; Fig. 5b). Whole-brain analysis (Fig. 5c) further substantiated this finding, as even after whole-brain correction, BOLD responses in the vmPFC remained significantly higher for non-smokers compared to smokers ($P_{FDR} < 0.05$,

$k > 50$). Overall, these results indicate aberrant neural encoding for the computation of FT values in the vmPFC in smokers.

Reduced midbrain tracking of norm prediction errors (nPEs) in smokers

We additionally evaluated nPEs encoding, given prior evidence of altered learning in smokers[24] and that role of nPEs norm updating within this task. Norm prediction errors, defined as the difference between the actual social (i.e. proposed offer) and one's expectation (i.e. internal norms). Based on previous research[25,26] implicating the of mesolimbic structures (e.g., midbrain) in reward-based learning, we extracted neural signals tracking nPEs using an independent ROI of midbrain [4, −26, −11] (Fig. 5d) encompassing regions of the ventral tegmental area and substantia nigra[27]. We found that while nPEs positively scaled with midbrain activity in non-smokers (parameter estimate: 0.302 ± 1.10), this relationship was inversed in smokers (parameter estimate: −0.306 ± 1.04; two-sample $t(40) = -1.80$, $p = 0.040$; Cohen's $d = 0.57$; Fig. 5e). Whole brain analysis further confirmed this significant group difference, with smokers exhibiting reduced activation compared to non-smokers in midbrain activity associated with nPEs (Fig. 5f; $P_{FDR} < 0.05$ and $k > 50$). Collectively, these results are consistent with previous findings indicating prediction error encoding deficits in smokers and extend beyond previous findings by elucidating how nicotine addiction is also associated with unusual updating of information in the context of dynamic social interactions[28–30].

Discussion

Social controllability, the ability to exert control during social interactions, is crucial for behavioral adaptability. Previous research suggests that accurately simulating the impact of one's actions on future states is crucial for exerting social influence, a process subserved by a vmPFC circuit[1,31]. Here, we examined how neural computation of social controllability might be altered in nicotine addiction. Our main finding suggested that, in a controllable social environment, smokers underestimated the downstream influence of their current choices and thus, failed to exploit the controllability of their social interactions. These behavioral and computational findings were replicated in an independent online sample of smokers and non-smokers. Neurally, smokers exhibited reduced encoding of forward thinking values in the vmPFC and reduced tracking of norm prediction errors in the midbrain. Collectively, these results suggest that social cognitive challenges in addiction might be associated with complex decision processes involving future-oriented thinking.

Previous work has often focused on how individuals with Substance Use Disorder (SUD) exert control over motor impulses or over actions with immediate outcomes, identifying reduced cognitive control and high impulsivity levels in these individuals[32–35]. Based on this body of literature, one might expect that smokers would exhibit a reduced planning horizon as suggested by previous computational work[6,36]. However, formal model comparison in our study showed that smokers engaged a similar 2-step forward thinking model as non-smoking controls yet underestimated the influence of their actions on future states (lower δ value) compared to non-smokers. This interpretation is consistent with the participants' subjective assessment of controllability in the game, wherein smokers indicated they perceived future offers as being less affected by their actions, compared to non-smokers. These findings support the notion that it is maladaptive for an agent to infer that they have less impact on the future than they actually do, as it may lead to missed exploitable opportunities and failure to avoid negative future consequences[37]. Although no punishment was introduced as outcome in our study design, our work provides a computational framework and paradigm that could be used by future research to examine mental simulation of future negative consequences. It also remains to be investigated whether the findings of smokers' underestimation of their influence is associated with a mismatch between available cognitive resources and environmental complexity[18,19].

Our finding aligns with and provides a computational explanation for the observed greater temporal discounting of future rewards in SUD[7–9], as well as findings suggesting that cognitive strategies involving deliberation and mental imagery of future events can reduce temporal discounting and cigarette consumption[38]. Although the temporal discounting parameter was fixed in our model setup due to technical considerations, our study expands this literature by showing that future-oriented valuation of one's own agency (i.e., calculating the impact of one's action on future events) is altered in smokers. This disruption may play a key role in their altered estimation of future values, contributing to the temporal discounting effect. These insights introduce new avenues for intervention, as an accurate prediction of how current actions impact future outcomes may help individuals with SUD reevaluate drug-related choices.

The cognitive deficit in forward thinking observed in smokers was corroborated by our neural finding of reduced activity in the vmPFC in tracking projected total choice value in this group. The vmPFC has been heavily implicated in both addiction[39–41] and value-based decision-making[1,29,42,43]. Specifically, decreased vmPFC activity has been associated with a reduced preference for delayed rewards and impairments in valuation processes[44–46]. In both occasional and nicotine-dependent smokers, activity in the mPFC is associated with decisions to purchase or consume cigarettes[47]. Here, we observed that vmPFC activity was in fact anticorrelated with projected total values in smokers, deviating from the positive association between the two measures observed in non-smokers. This finding, along with past research, demonstrates that deficit in the vmPFC is associated with suboptimal decision-making in nicotine addiction. Our result also expands beyond previous work by demonstrating that aberrant neural activity in the vmPFC is detrimental to not only value representation but also future-oriented, model-based planning. This finding is consistent with more recent work highlighting the role of vmPFC in representing states and task structure[20,48].

We also found aberrant neural tracking of norm prediction errors in the midbrain in smokers. Norm prediction errors, defined as the difference between the actual social signal (i.e., proposed offer) and one's expectation (i.e., internal norms), allows an agent to flexibly adapt to a changing social environment where norms could fluctuate. Previously, activities in midbrain structures – including the substantia nigra and ventral tegmental area-have been linked to social norm updating and decision-making during the ultimatum game[49]. Existing work has also indicated altered non-social reward prediction error encoding in individuals with addiction[30,50]. Hence, we extend both lines of previous work by suggesting that addiction is also linked to neural deficits in the midbrain during aberrant norm updating in complex social environments.

Finally, despite the acknowledgment of the importance of social factors in addiction[51], very little empirical evidence exists that explain how social cognition is impacted in nicotine-dependent participants at either the neural or the computational level. In one study, Chung and colleagues used a peer influence paradigm and fMRI[21] in adolescents; they found that substance naïve teens showed enhanced vmPFC activations towards safe choices made by peers, compared to teens who had used substances[52]. This result suggests that substance use might be associated with reduced ability to distinguish benevolent vs. malevolent social signals. In this sense, our work expands our knowledge about the social brain in SUD in suggesting that in addition to biased social perception, impaired social learning and inability to exert control during interpersonal interactions are also features of SUD.

Limitations of the current study include a small sample size and low representation of females in the fMRI study due to sex imbalances associated with nicotine addiction[53,54]. As such, further larger-scale studies are needed to address the potential sex differences in nicotine addiction-related neural mechanisms and to provide more conclusive insights. Furthermore, although we were able to demonstrate group differences between smokers and controls, we were not able to carry out the planned analysis on how craving status might affect social controllability computations, as our

attempt of instructing smokers to stay abstinent overnight failed in the experiment (see *Methods*). Future studies may investigate the relationship between deprivation level and social decision-making by using experimental designs that can more effectively vary participants' abstinence and craving levels. Lastly, while participants were informed that they were playing with simulated players, we did not track their beliefs about the "humanness" of the other players. Future work could explicitly measure such belief and examine how it might affect participants' social choices.

In conclusion, our findings suggest that under-estimation of the future consequences of their choices may be a key feature of nicotine-dependent humans and contribute to their inability to exert control in social settings. This serves as a plausible neurocomputational account for the social cognitive deficits observed in this population.

Methods

Participants

In-person fMRI study. The fMRI study was approved by the Institutional Review Board (IRB) of the University of Texas at Dallas and the University of the Texas Southwestern Medical Center (where SN, MH, VFG, and XG worked and collected this dataset). All participants were recruited from the Dallas-Fort Worth metropolitan area through advertisements and flyers. All participants provided written informed consent before participating in the study and were compensated based on time and task performance (i.e., the outcome of a randomly drawn trial). All ethical regulations relevant to human research participants were followed. The criteria for in-person smoker recruitment included participants who smoked more than 10 cigarettes daily for at least a year and were fluent in English. All candidate participants underwent Structured Clinical Interview for DSM Disorders (SCID) – substance use disorder (SUD) module. For all participants, the exclusion criteria were any major medical, neurological, or psychiatric conditions; any incompatibility with MRI safety (e.g., metal implants); and dependence on substances other than nicotine and alcohol (smokers) or any substance dependance (non-smokers). In the final sample, smokers had a mean daily consumption of 18 cigarettes, and mean baseline carbon monoxide (CO) level of 15.59 (SD: 8.89) parts per million (ppm). A total of 25 non-smoking and 17 nicotine-smoking participants were included in the final fMRI sample (Table S1). The fMRI study was pre-registered as part of a larger fMRI study examining decision-making in smokers (https://osf.io/m9cws).

Online study. The online study was approved by the IRB of the Icahn School of Medicine at Mount Sinai. We recruited U.S.-based participants from the online participant pool Prolific (http://prolific.co). Here, we included a wider range of smokers (smoked at least one cigarette per week) to examine if findings from the in-person sample whose nicotine addiction was severe might generalize to a more representative sample of smokers with a wider range of nicotine dependence levels. Smokers with self-reported medical or psychiatric diagnosis were excluded. The final online smoker sample ($n = 72$) had a mean daily tobacco consumption of 9.34 and had a mean craving score of 64.51 out of 100. All participants provided online consent before participating in the study and were compensated for their time. The criteria for online non-smokers included zero tobacco consumption, no cravings for tobacco in the past week, and no major medical or psychiatric diagnoses. A total of 147 online participants met these criteria for non-smokers and were matched with online smokers for sex, age, education, and handedness (Table S2). This online study was pre-registered as a subcomponent of a larger longitudinal study investigating social decision-making (https://osf.io/8s5mu).

Study procedure

For the in-person study, all candidate participants underwent Structured Clinical Interview for DSM Disorders (SCID) – substance use disorder module, which was used to determine if they had nicotine addiction and/or other comorbid substance use disorder. For smokers, we also measured their exhaled CO levels using a smokerylzer (Covita Smokerlyzer) and administered a battery of questionnaires on their demographics and smoking habits. Specifically, the Shiffman-Jarvik Withdrawal Scale[55] was used to assess participants' craving and withdrawal symptoms. Non-smokers completed a survey of their demographics. Participants were then asked to withdraw from smoking 12 h prior to the next scheduled visit. However, CO levels measured on the day of scanning suggested that smokers were likely to have smoked regardless and failed to stay abstinent as instructed. As such, we were unable to conduct planned analyses on how craving affected social controllability per our preregistration.

Participants played a two-party exchange task in a Phillips 3T MRI. A Phillips 3T MRI scanner was used to obtain anatomical and functional images of participants completing the task. High-resolution structural images were collected using a multi-echo MP-RAGE sequence with the following parameters: TR/TE/TI = 2300/2.74/900 ms, flip angle = 8°, FOV = 256 × 256 mm, Slab thickness = 176, Voxel size = 1 × 1 × 1 mm, Number of echos = 4, Pixel bandwidth = 650 Hz, Total scan time = 6 min. These structural scans were used for alignmemnt of images. fMRI scans were obtained by setting repetition time (TR) to 2000 ms, echo time (TE) to 25 ms, voxel size to 3.4 mm × 3.4 mm × 4.0 mm, flip angle to 90°, and slice number to 37.

For the online study, after participants consented for research, they completed a battery of surveys that assessed demographics, mental health, and substance use as well as the social controllability task, as described below.

Social controllability task

All participants completed a two-party exchange task[1] adapted from the ultimatum game in which simulated partners proposed how to divide a sum of $20 and participants decided whether to accept or reject the offer. If the participant accepted the offer, both the responder (participant) and the proposer received the proposed amount as is. If the participant rejected the offer, neither party received a reward. Offers were always disadvantageous to the participant/responder (<= $9) and the initial offer was always $5 ("indifference point").

Importantly, we modified the game so that participants could influence their partner's future monetary proposal using their current actions[1] (Fig. 1). Specifically, if participants rejected the current offer, the next offer would increase by $0, $1 or $2 with a 1/3 probability for each option; and if they accepted the current offer, the next one would decrease by $0, $1 or $2 with a 1/3 probability for each (Fig. 1b). We also included a typical ultimatum game block in which the offer was randomly drawn from normal distribution with a mean of $5 and participants' current choice to accept or reject the offer had no influence over the future offers ("uncontrollable" condition; see Supplementary Fig. S1).

Participants were told that they were playing with members of two different teams and were not given explicit information regarding how the two teams might differ. Instead, they were instructed that they "may or may not have influence over the offers made" by the team. The order of the conditions was counterbalanced. The original task with non-smokers included 40 trials per condition and smokers played a slightly shorter version of 30 trials that were shown to generate similar results[1]. Nevertheless, to match the task length between smokers and non-smokers, only the first 30 trials from non-smoker data were included in the analyses. The number of trials of the game was unknown to the participant. After completing the task, participants were asked to rate their perceived influence over their partners' offers at the end of each condition using a scale from 0 to 100 ("perceived controllability). One outcome from all trials was randomly selected as a bonus payment to incentivize participants in both the fMRI and the online sample. The social controllability task was pre-registered as a subcomponent of a larger project investigating value-based decision making in nicotine addiction (https://osf.io/m9cws).

Computational modeling of choice behavior

The *forward thinking (FT) value*, or mentally projected total value of an action taken at the ith trial, $v|_{a_i}$, (a_i, *acceptance or rejection*) is estimated in an n-step forward thinking model, which considers various planning horizons given hypothetical future actions. Here the FT value $v|_{a_i}$ takes into

account both current and future utilities of a choice.

$$v|_{a_i} = U(r_i, f_i) + \sum_{j=1}^{n} \gamma^j \times U\left(\hat{E}(r_{i+j}|a_i, \underline{a}_{i+1}, \ldots \underline{a}_{i+j}), f_i\right)$$

Current utility $U(r_i, f_i)$ is a function of reward r_i and internal norm f_i at the ith trial, defined as follows:

$$U(r_i, f_i) = \begin{cases} r_i - \alpha \max[f_i - r_i, 0] & \text{if } r_i > 0 \text{ (accepted)} \\ 0 & \text{if } r_i = 0 \text{ (rejected)} \end{cases}$$

The degree of aversion or sensitivity to norm violation at the individual level is captured by α $(0 \le \alpha \le 1)$[56]. Internal norm f_i is a measure of subjective norm, or one's trial-by-trial expectation of the offer. Here, we assumed that participants update their internal representation of the norm from trial to trial using the Rescorla-Wagner learning model based on our previous work[57] and that the initial norm f_0 varies from individual to individual with a range of [$0, $20][43].

$$f_i = f_{i-1} + \varepsilon(s_i - f_{i-1})$$

Here the learning rate ε $(0 \le \varepsilon \le 1)$ represents how fast one updates expectation of the offer based on the *norm prediction error* (nPE), defined as $(s_i - f_{i-1})$.

Future utility is described as the summed utility of the mentally simulated future actions $\underline{a}$ discounted by γ, the temporal discounting factor. Similar to our previous work, we fixed γ at 0.8, the mean value measured in a larger cohort to control for collinearity with our parameter of interest δ[1]. $\hat{E}$ is the subject's mentally simulated future split. Importantly, our parameter of interest δ represents how much (in dollar amount) a participant thought their action changed the partner's proposed split at a future trial, $\underline{a}_k$, in the following manner:

$$\hat{E}(s_{k+1}) = \begin{cases} s_k + \delta & \text{if } a_k \text{ or } \underline{a}_k = 0 \\ \max(s_k - \delta,\ 1) & \text{if } a_k \text{ or } \underline{a}_k = 1 \end{cases}$$

$$\underline{a}_k = \begin{cases} 1 \text{ if } U\left(\hat{E}(s_k), f_k\right) > 0 \\ 0 \qquad \text{otherwise} \end{cases}$$

Critically, δ represents a subject's mentally *estimated influence* of their current action on the subsequent offer (in dollar amount, ranging from $-\$2 \le \delta \le \$2$)). The simulated future action $\underline{a}_k$ of accepting an offer is determined by the subjective utility of the following rewards $U(\hat{E}(s_k), f_k)$. In the event that the simulated chosen action is to accept the offer ($\underline{a}_k = 1$), the hypothetical next offer $\hat{E}(s_{k+1})$ decreases by the *estimated influence* parameter δ ($-\$2 \le \delta \le \$2$). In the event that the simulated chosen action is to reject the offer ($\underline{a}_k = 0$) the hypothetical next offer $\hat{E}(s_{k+1})$ increases by δ. Here δ is applied symmetrically to acceptance and rejection, also similar to our previous work[1,58].

Action selection was based on the difference between the total projected value of accepting an offer ($v|_{a_i=1}$) and the total projected value of rejecting an offer ($v|_{a_i=0}$).

$$\Delta Q_i = v|_{a_i=1} - v|_{a_i=0}$$

ΔQ_i in turn influences the probability of choosing an action in a softmax function:

$$P_i(a_i = 1) = \frac{e^{\beta \Delta Q_i}}{1 + e^{\beta \Delta Q_i}}$$

Behavioral responses were fitted into five models, each incorporating different planning horizons: 0-step, 1-step, 2-step, 3-step, 4-step. The 0-step model represents a standalone norm learning model and excludes any forward thinking. The other four models assume that an agent simulates the value of an action by considering both current and future values, all based upon the estimated levels of controllability of the social environment. We additionally fitted a model-free RL model which only considers cached values (see Supplementary Information for details). The best fitting model was chosen based on both Deviation Information Criteria (DIC) (where a smaller index indicates both higher model evidence and lower model complexity; see Table S3) and the recoverability of model parameters (see Tables S4, S5).

Individual choices from middle trials (trials 6–25) were used for model fitting. The first 5 trials were excluded from all participants' data to allow behavior to stabilize after participants explored the contingencies of the task in these initial trials. The last 5 trials from the smokers' responses were also excluded given that there was less incentive to reject offers closer to the end of the game[39]. Finally, the last 15 trials from the non-smokers' responses were excluded in order to keep a consistent trial number with the smokers during analysis. The computational models were also pre-registered as a subset of the project examining value-based decision making in nicotine addiction (https://osf.io/m9cws).

Statistics and reproducibility

Our analyses focused on group comparisons between smokers and non-smokers, per our pre-registrations. For statistical tests, we first examined if our key measures and parameters of interest met the criteria for standard parametric tests. We found that the total rejection rate for online non-smoker participants ($n = 147$) exhibited a Kolmogrov–Smirnov (K–S) test statistic (D) of 0.20015 where p is 0.0001, indicating strong evidence that rejection rates were not normally distributed. Similarly, parameter values from the model also deviate from a normal distribution, as demonstrated by delta for all online participants with a K–S test statistic (D) of 0.21002, $p < 0.00001$. In light of this evidence as well as the highly unbalanced sample sizes of the online study, we used a non-parametric bootstrapping method following previous work conducted with similar constraints[43,59–61] to assess the probability of observing a difference between two groups. Therefore, a bootstrapping method was employed to compare all online parameters between smokers and non-smokers, while a 2-sample t-test was used to compare fMRI in-person parameters between the two groups.

The bootstrapping procedure was conducted with 10,000 iterations as follows (e.g., the comparison between 72 smokers and 147 non-smokers): (i) 72 participants were selected randomly as the surrogate smoker group, from the whole group of 219 online participants including both smokers and non-smokers; (ii) 147 participants were selected randomly as the surrogate non-smoker group from the whole group of 219 participants; and (iii) the two-tailed t-value of the difference between the two surrogate groups was calculated. After 10,000 iterations, the distribution of the t-values was obtained. The observed t-value (e.g., between smoker and non-smoker groups) was then calculated and compared along the t distribution. If the probability of obtaining the observed t-value along the permutated distribution of t-value is <5% (one tailed), we considered the difference between the patient and control groups to be significant.

We applied additional general linear modeling to further explore the effects of negative mood and impulsivity on the model estimated controllability (Tables S6, S7). Similar regression approach is applied to explore the effect of risk aversion on smokers and non-smokers' choice behavior measured as rejection rates (Tables S8, S9). Analyses were performed using MATLAB (2020b)[62], R 4.3.1[63], and RStudio 2023.6.0.42[64]. MATLAB was used for data management. R and RStudio were used for data curation and regression analysis using the *lme4* package[65].

For reproducibility, our focus was mainly twofold. First, we replicated the key behavioral and computational findings in an independent group of smokers and non-smokers recruited online, as described in previous

sections. The replication sample was much larger ($n = 219$ in total) than the original fMRI group ($n = 42$) and more heterogenous, yet still replicating all major findings and confirming our original hypothesis. Second, we have made our data and code publicly available through GitHub (https://github.com/caromc03/Smoker-s-Forward-Thinking; also see Data and Code Availability section below).

fMRI data analysis

The functional scans were analyzed using the statistical parametric mapping software package (SPM12, Wellcome Department of Imaging Neuroscience; www.fil.ion.ucl.ac.uk/spm). First, we preprocessed the images by implementing time correction, co-registration, and normalization with resampled voxel size of 2 mm × 2 mm × 2 mm and smoothing with an 8 mm Gaussian kernel. After preprocessing, two general linear models (GLMs) were constructed using SPM12 to examine the neural correlates of (1) forward thinking value and (2) norm prediction errors (PEs). The following event regressors were included: (1) offer onset, (2) choice submission, (3) outcome onset, and (4) perceived controllability rating.

Importantly, we specified a parametric modulator of FT value, the forward projected choice value from the 2-step model, normalized at the individual level, at the onset of choice submission. A separate GLM was conducted in which the learning signal nPE replaced the total choice values as the parametric regressor. In both GLMs, six motion parameters were included as covariates. Following individual model estimation at the 1st (subject) level, contrast images representing either total choice value or norm PE were entered into an ANOVA test to compare neural differences between smokers and non-smokers ($P_{FDR} < 0.05$ and $k > 50$).

We used the MarsBar toolbox[66] to conduct region of interest (ROI) analyses. Beta values representing choice value-related activations were extracted from an 8-mm radius sphere of the vmPFC using coordinates [−2, 50, −2] from an independent study[23]. Beta values representing norm PE were extracted at a coordinate of the midbrain [−4, −26, −11] on an 8-mm radius sphere, from an independent study[27]. The ROI in the analyses were specified in the pre-registered study (https://osf.io/m9cws).

Reporting summary

Further information on research design is available in the Nature Portfolio Reporting Summary linked to this article.

Data availability

All source data used for this manuscript can be accessed in Supplementary Data 1 and in the following link: https://github.com/caromc03/Smoker-s-Forward-Thinking.

Code availability

All code used for this manuscript can be accessed here: https://github.com/caromc03/Smoker-s-Forward-Thinking.

Received: 11 January 2024; Accepted: 26 July 2024;
Published online: 14 August 2024

References

1. Na, S. et al. Humans use forward thinking to exploit social controllability. *eLife* **10**, e64983 (2021).
2. Moran, S., Wechsler, H. & Rigotti, N. A. Social smoking among US college students. *Pediatrics* **114**, 1028–1034 (2004).
3. Waters, K., Harris, K., Hall, S., Nazir, N. & Waigandt, A. Characteristics of social smoking among college students. *J. Am. Coll. Health* **55**, 133–139 (2006).
4. Mollick, J. A. & Kober, H. Computational models of drug use and addiction: a review. *J. Abnorm. Psychol.* **129**, 544–555 (2020).
5. Redish, A. D. Addiction as a computational process gone awry. *Science* **306**, 1944–1947 (2004).
6. Redish, A. D., Jensen, S. & Johnson, A. A unified framework for addiction: vulnerabilities in the decision process. *Behav. Brain Sci.* **31**, 415–437 (2008).
7. Audrain-McGovern, J. et al. Does delay discounting play an etiological role in smoking or is it a consequence of smoking? *Drug Alcohol Depend.* **103**, 99 (2009).
8. Johnson, M. W., Bickel, W. K. & Baker, F. Moderate drug use and delay discounting: a comparison of heavy, light, and never smokers. *Exp. Clin. Psychopharmacol.* **15**, 187–194 (2007).
9. Reynolds, B., Richards, J. B., Horn, K. & Karraker, K. Delay discounting and probability discounting as related to cigarette smoking status in adults. *Behav. Process.* **65**, 35–42 (2004).
10. Anderhub, V. & Güth, W. On the interaction of risk and time preferences: an experimental study. *Ger. Econ. Rev.* **2**, 239–253 (2001).
11. Lopez-Guzman, S., Konova, A. B., Louie, K. & Glimcher, P. W. Risk preferences impose a hidden distortion on measures of choice impulsivity. *PloS ONE* **13**, e0191357 (2018).
12. Traeger, C. P. Once upon a time preference - How rationality and risk aversion change the rationale for discounting. Report No. ID 2045990, (Social Science Research Network, Rochester, NY, 2012).
13. Dolan, R. J. & Dayan, P. Goals and habits in the brain. *Neuron* **80**, 312–325 (2013).
14. Sebold, M. et al. When habits are dangerous: alcohol expectancies and habitual decision making predict relapse in alcohol dependence. *Biol. Psychiatry* **82**, 847–856 (2017).
15. Redish, A. D. & Johnson, A. A computational model of craving and obsession. *Ann. N. Y. Acad. Sci.* **1104**, 324–339 (2007).
16. Shimomura, K., Kato, A. & Morita, K. Rigid reduced successor representation as a potential mechanism for addiction. *Eur. J. Neurosci.* **53**, 3768–3790 (2021).
17. Simon, D. A. & Daw, N. D. in *Computational Neuroscience of Drug Addiction Springer Series in Computational Neuroscience* (eds Gutkin B & Ahmed, S. H.) 145−161 (Springer, 2012).
18. Fiore, V. G., Ognibene, D., Adinoff, B. & Gu, X. A Multilevel computational characterization of endophenotypes in addiction. *eNeuro* **5**, ENEURO.0151-0118.2018. https://doi.org/10.1523/ENEURO.0151-18.2018 (2018).
19. Ognibene, D., Fiore, V. G. & Gu, X. Addiction beyond pharmacological effects: the role of environment complexity and bounded rationality. *Neural Netw.* **116**, 269–278 (2019).
20. Schuck, N. W., Cai, M. B., Wilson, R. C. & Niv, Y. Human orbitofrontal cortex represents a cognitive map of state space. *Neuron* **91**, 1402–1412 (2016).
21. Chung, D., Christopoulos, G. I., King-Casas, B., Ball, S. B. & Chiu, P. H. Social signals of safety and risk confer utility and have asymmetric effects on observers' choices. *Nat. Neurosci.* **18**, 912–916 (2015).
22. Bernoulli, D. Exposition of a new theory on the measurement of risk. *Econometrica* **22**, 23–36 (1954).
23. D'Argembeau, A. et al. Valuing one's self: medial prefrontal involvement in epistemic and emotive investments in self-views. *Cereb. Cortex* **22**, 659–667 (2011).
24. Baker, T. E., Zeighami, Y., Dagher, A. & Holroyd, C. B. Smoking decisions: altered reinforcement learning signals induced by nicotine state. *Nicotine Tob. Res.* **22**, 164–171 (2020).
25. Fischbach, S. & Janak, P. H. Decreases in cued reward seeking after reward-paired inhibition of mesolimbic dopamine. *Neuroscience* **412**, 259–269 (2019).
26. Hauser, T. U., Eldar, E. & Dolan, R. J. Separate mesocortical and mesolimbic pathways encode effort and reward learning signals. *Proc. Natl Acad. Sci.* **114**, E7395–E7404 (2017).
27. Murty, V. P. et al. Selective updating of working memory content modulates meso-cortico-striatal activity. *NeuroImage* **57**, 1264–1272 (2011).

28. Gu, X. et al. Belief about nicotine selectively modulates value and reward prediction error signals in smokers. *Proc. Natl Acad. Sci.* **112**, 2539–2544 (2015).
29. Piña, J. A., Namba, M. D., Leyrer-Jackson, J. M., Cabrera-Brown, G. & Gipson, C. D. in *International Review of Neurobiology* Vol. 140 *Animal Models for Examining Social Influences on Drug Addiction* (eds Olive, F. M. & Tomek, S. E.) 1−32 (Academic Press, 2018).
30. Tolomeo, S., Yaple, Z. A. & Yu, R. Neural representation of prediction error signals in substance users. *Addctn. Biol.* **26**, e12976 (2021).
31. Na, S., Rhoads, S. A., Yu, A. N. C., Fiore, V. G. & Gu, X. Towards a neurocomputational account of social controllability: from models to mental health. *Neurosci. Biobehav. Rev.* **148**, 105139 (2023).
32. Dakhili, A. et al. Cue-induced craving and negative emotion disrupt response inhibition in methamphetamine use disorder: Behavioral and fMRI results from a mixed Go/No-Go task. *Drug Alcohol Depend.* **233**, 109353 (2022).
33. Franken, I. H. A., van Strien, J. W., Nijs, I. & Muris, P. Impulsivity is associated with behavioral decision-making deficits. *Psychiatry Res.* **158**, 155–163 (2008).
34. Izquierdo, A. & Jentsch, J. D. Reversal learning as a measure of impulsive and compulsive behavior in addictions. *Psychopharmacology* **219**, 607–620 (2012).
35. Silva, G. M. et al. Does chronic smoking affect performance on a go/no-go task? *Curr. Psychol.* https://doi.org/10.1007/s12144-020-01305-y (2021).
36. Kato, A. et al. Computational models of behavioral addictions: state of the art and future directions. *Addctn. Behav.* **140**, 107595 (2023).
37. Ligneul, R. Prediction or Causation? Towards a redefinition of task controllability. *Trends Cogn. Sci.* **25**, 431–433 (2021).
38. Stein, J. S., Tegge, A. N., Turner, J. K. & Bickel, W. K. Episodic future thinking reduces delay discounting and cigarette demand: an investigation of the good-subject effect. *J. Behav. Med.* **41**, 269–276 (2018).
39. Gneezy, U., Haruvy, E. & Roth, A. E. Bargaining under a deadline: evidence from the reverse ultimatum game. *Games Econ. Behav.* **45**, 347–368 (2003).
40. Janes, A. C., Farmer, S., Frederick, B. D., Nickerson, L. D. & Lukas, S. E. An increase in tobacco craving is associated with enhanced medial prefrontal cortex network coupling. *PLOS ONE* **9**, e88228 (2014).
41. Konova, A. B. et al. Neural mechanisms of extinguishing drug and pleasant cue associations in human addiction: role of the VMPFC. *Addctn. Biol.* **24**, 88–99 (2019).
42. Fellows, L. K. & Farah, M. J. The role of ventromedial prefrontal cortex in decision making: judgment under uncertainty or judgment per se? *Cereb. Cortex* **17**, 2669–2674 (2007).
43. Gu, X. et al. Necessary, yet dissociable contributions of the insular and ventromedial prefrontal cortices to norm adaptation: computational and lesion evidence in humans. *J. Neurosci.* **35**, 467–473 (2015).
44. Balodis, I. M. et al. Diminished frontostriatal activity during processing of monetary rewards and losses in pathological gambling. *Biol. Psychiatry* **71**, 749–757 (2012).
45. Noda, Y. et al. Neural correlates of delay discount alterations in addiction and psychiatric disorders: a systematic review of magnetic resonance imaging studies. *Prog. Neuro-Psychopharmacol. Biol. Psychiatry* **99**, 109822 (2020).
46. Schüller, C. B., Kuhn, J., Jessen, F. & Hu, X. Neuronal correlates of delay discounting in healthy subjects and its implication for addiction: an ALE meta-analysis study. *Am. J. Drug Alcohol Abus.* **45**, 51–66 (2019).
47. Lawn, W. et al. Value-based decision-making of cigarette and nondrug rewards in dependent and occasional cigarette smokers: an FMRI study. *Addctn. Biol.* **25**, e12802 (2020).
48. Zhou, J. et al. Complementary task structure representations in hippocampus and orbitofrontal cortex during an odor sequence task. *Curr. Biol.* **29**, 3402–3409.e3403 (2019).
49. Hétu, S., Luo, Y., D'Ardenne, K., Lohrenz, T. & Montague, P. R. Human substantia nigra and ventral tegmental area involvement in computing social error signals during the ultimatum game. *Soc. Cogn. Affect. Neurosci.* **12**, 1972–1982 (2017).
50. Redish, A. D., Jensen, S., Johnson, A. & Kurth-Nelson, Z. Reconciling reinforcement learning models with behavioral extinction and renewal: Implications for addiction, relapse, and problem gambling. *Psychol. Rev.* **114**, 784–805 (2007).
51. Leach, D. & Kranzler, H. R. An interpersonal model of addiction relapse. *Addict. Disord. Treat.* **12**, 183 (2013).
52. Chung, D., Orloff, M. A., Lauharatanahirun, N., Chiu, P. H. & King-Casas, B. Valuation of peers' safe choices is associated with substance-naïveté in adolescents. *Proc. Natl Acad. Sci.* **117**, 31729–31737 (2020).
53. Higgins, S. T. et al. A literature review on prevalence of gender differences and intersections with other vulnerabilities to tobacco use in the United States, 2004-2014. *Prevent. Med.* **80**, 89–100 (2015).
54. Jamal, A. et al. Current cigarette smoking among adults - United States, 2005-2015. *Mmwr. Morbid. Mortal. Wkly. Rep.* **65**, 1205–1211 (2016).
55. Shiffman, S. M. & Jarvik, M. E. Smoking withdrawal symptoms in two weeks of abstinence. *Psychopharmacology* **50**, 35–39 (1976).
56. Fehr, E. & Schmidt, K. M. A theory of fairness, competition, and cooperation. *Q. J. Econ.* **114**, 817–868 (1999).
57. Sutton, R. S. & Barto, A. G. *Reinforcement learning: An introduction*. 2nd ed (The MIT Press, 2018).
58. Na, S. et al. Computational mechanisms underlying illusion of control in delusional individuals. *Schizophr. Res*. https://doi.org/10.1016/j.schres.2022.01.054 (2022).
59. Hasson, U., Avidan, G., Deouell, L. Y., Bentin, S. & Malach, R. Face-selective activation in a congenital prosopagnosic subject. *J. Cogn. Neurosci.* **15**, 419–431 (2003).
60. Gu, X. et al. Anterior insular cortex is necessary for empathetic pain perception. *Brain* **135**, 2726–2735 (2012).
61. Mooney, C. Z. & Duval, R. D. *Bootstrapping: A Nonparametric Approach to Statistical Inference*. (Sage Publications, 1993).
62. The MathWorks Inc. MATLAB. Version 2020a. The MathWorks Inc. (2020). Available at: http://www.mathworks.com.
63. R Core Team (2023). _R: A Language and Environment for Statistical Computing_. R Foundation for Statistical Computing, Vienna, Austria. https://www.R-project.org/
64. Posit team. RStudio: Integrated Development Environment for R. Posit Software, PBC, Boston, MA. http://www.posit.co/ (2023).
65. Bates, Douglas, Maechler, Martin, Bolker, Ben & Walker, Steve Fitting linear mixed-effects models using lme4. *J. Stat. Softw.* **67**, 1–48 (2015).
66. Brett, M., Anton, J.-L., Valabregue, R. & Poline, J.-B. Region of interest analysis using an SPM toolbox [abstract]. Presented at the 8th International Conference on Functional Mapping of the Human Brain, June 2–6, 2002, Sendai, Japan. NeuroImage 16, abstract 497 (2002). Available on CD-ROM.

Acknowledgements

We thank the staff members at the UT Southwestern Imaging Center for their assistance with scanning. This study was funded by internal funding from the University of Texas, Dallas where X.G. worked. X.G. is funded by the National Institute on Drug Abuse [grant numbers: R01DA043695, R21DA049243]. The funders had no role in study design, data collection and analysis, decision to publish, or preparation of the manuscript. This work represents the Master's thesis of Caroline McLaughlin as a partial requirement for the fulfillment of the MS degree in Biomedical Sciences offered by the Graduate School of Biomedical Sciences at Mount Sinai.

Author contributions

Caroline McLaughlin: Formal analysis, Visualization, Writing – original draft; Writing - review and editing. Soojung Na: Data curation, Investigation, Methodology, Software. Matthew Heflin: Data curation, Investigation,

Project Administration. Dongil Chung: Data curation, Supplementary Analysis. Qi Xiu Fu: Data curation, Supplementary Analysis, Writing - review and editing. Vincenzo G. Fiore: Conceptualization, Writing - review & editing. Xiaosi Gu: Conceptualization, Funding acquisition, Methodology, Project Administration, Resources, Supervision Writing - review and editing.

Competing interests
The authors declare no competing interests.

Ethics approval
All fMRI participants provided written informed consent and all online participants provided online consent. The fMRI study was approved by the Institutional Review Board of the University of Texas at Dallas (IRB 15-77) and the University of the Texas Southwestern Medical Center (STU 072015-031) (S.N., V.G.F, and X.G.'s previous institute where data were collected). Analyses of the original fMRI data collected at UT Dallas were covered by a Data Use Agreement between UT Dallas and the Icahn School of Medicine at Mount Sinai (ISMMS) (#19C7073) and IRB protocol approved by the ISMMS (HS#: 18-00728). The online study was approved by the Institutional Review Board at the Icahn School of Medicine at Mount Sinai (determined exempt; IRB-18-01301).

Additional information
Supplementary information The online version contains supplementary material available at https://doi.org/10.1038/s42003-024-06638-z.

Correspondence and requests for materials should be addressed to Xiaosi Gu.

Peer review information *Communications Biology* thanks Silvia Lopez-Guzman and the other, anonymous, reviewer(s) for their contribution to the peer review of this work. Primary Handling Editors: Joao Valente. A peer review file is available.